Do photon-induced processes survive in semi-central heavy-ion collisions?

XIV Polish Workshop on Relativistic Heavy-Ion Collisions, Kraków, April 6-7 2019

Antoni Szczurek [1,2]

[1]Institute of Nuclear Physics PAN Kraków
[2]University of Rzeszów

Introduction

- J/ψ was known to be produced in heavy-ion collisions.
  Multiple NN collisions or from QGP.
- Photoproduction of vector mesons was known to occur in UPCs.
- ALICE observed J/ψ with very small transverse momenta also in peripheral and semi-central collisions.
- We interpreted this in 2016 as due to photoproduction of J/ψ which survives even there.
- However, the dependence on impact parameter is a bit complicated.
- Recently the STAR collaboration observed enhanced production of dielectron pairs with small transverse momenta.
- We show that this may be interpreted as $\gamma\gamma \to e^+e^-$ processes even in central collisions.

Our current analyses

The presentation will be based on our two analyses:

- M. Kłusek-Gawenda and A. Szczurek,
  "Photoproduction of J/ψ mesons in peripheral and semicentral heavy ion collisions",
  Phys. Rev. **C93** (2016) 044912.
- M. Kłusek-Gawenda, R. Rapp, W. Schäfer and A. Szczurek,
  "Dilepton Radiation in Heavy-Ion Collisions at Small Transverse Momentum",
  arXiv:1809.07049, Phys. Lett. **B790** (2019) 339.

Photoproduction of vector mesons

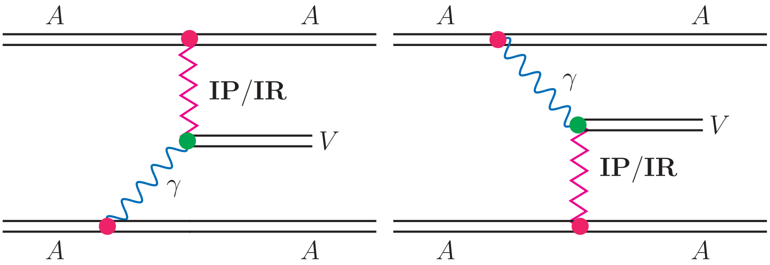

Figure: Schematic diagrams for the single vector meson production by photoproduction (photon-$\mathbb{P}/\mathbb{R}$ (left) or $\mathbb{P}/\mathbb{R}$-photon (right) fusion). Here the symbol $\mathbb{P}/\mathbb{R}$ is an abbreviation for multiple diffractive scattering of the hadronic system in the nuclear medium.

Photoproduction of vector mesons

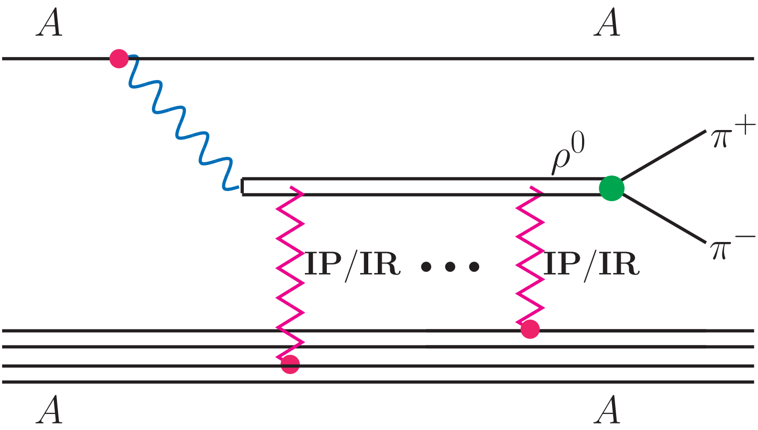

Some details of calculations for UPC

The cross section for this mechanism is usually written differentially in the impact parameter b and in the vector meson rapidity y

$$\frac{\mathrm{d}\sigma_{A_1A_2\to A_1A_2V}}{\mathrm{d}^2b\mathrm{d}y} = \frac{\mathrm{d}P_{\gamma\mathbf{P}/\mathbf{R}}(y,b)}{\mathrm{d}y} + \frac{\mathrm{d}P_{\mathbf{P}/\mathbf{R}\gamma}(y,b)}{\mathrm{d}y}\,. \tag{1}$$

Both exchange of Pomeron and Reggeon is possible in a general case of photoproduction of vector mesons. For J/ψ production the Reggeon exchange may be safely neglected.
In Eq.(1) $P_{\gamma\mathbf{P}/\mathbf{R}}(y,b)$ or $P_{\mathbf{P}/\mathbf{R}\gamma}(y,b)$ is the probability density for producing a vector meson V at rapidity y for fixed impact parameter b of the heavy-ion collision.

Some details of calculations for UPC

Each of the probabilities is the convolution of the cross section for $\gamma_1 A_2 \to VA_2$ or $\gamma_2 A_1 \to VA_1$ (the photon emitted from first ($\omega_1 = (m_V/2)\exp(+y)$) or second ($\omega_2 = (m_V/2)\exp(-y)$) nucleus and a corresponding flux of equivalent photons:

$$\frac{\mathrm{d}P_{\gamma\mathbf{P}/\mathbf{P}\gamma}(y,b)}{\mathrm{d}y} = \omega_{1/2} N\left(\omega_{1/2}, b\right) \sigma_{\gamma A_{2/1} \to VA_{2/1}}(W_{\gamma A_{2/1}}) S(b)\,, \qquad (2)$$

where $N\left(\omega_{1/2}, b\right)$ is usually a function of impact parameter between heavy ions (b) and not of photon-nucleus impact parameter. Finally $S(b)$ is an impact parameter dependent function which with good precision can be approximated by a geometrical factor $S(b) \approx \theta(b - R_A - R_B)$. In UPC's the geometrical factor excludes cases when nuclei collide, that at high-energies automatically means their break up.

Some details of the calculation

$$\sigma_{\gamma A \to J/\psi A} = \frac{\mathrm{d}\sigma_{\gamma A \to J/\psi A}}{\mathrm{d}t}|_{t=0} \int\limits_{-\infty}^{t_{max}} \mathrm{d}t \, |F_A(t)|^2 = \frac{\alpha_{em}}{4f^2_{J/\psi}} \sigma^2_{tot,J/\psi A} \int\limits_{-\infty}^{t_{max}} \mathrm{d}t \, |F_A(t)| \tag{3}$$

In our present calculations we use the following sequence of equations:

$$\frac{\mathrm{d}\sigma_{\gamma p \to J/\psi p}(t=0)}{\mathrm{d}t} = B_{J/\psi} X_{J/\psi} W_{\gamma p}^{\epsilon_{J/\psi}} , \tag{4}$$

$$\frac{\mathrm{d}\sigma_{J/\psi p \to J/\psi p}(t=0)}{\mathrm{d}t} = \frac{f^2_{J/\psi}}{4\pi\alpha_{em}} \frac{\mathrm{d}\sigma_{\gamma p \to J/\psi p}(t=0)}{\mathrm{d}t} , \tag{5}$$

$$\sigma^2_{tot,J/\psi p} = 16\pi \frac{\mathrm{d}\sigma_{J/\psi p \to J/\psi p}(t=0)}{\mathrm{d}t} , \tag{6}$$

Some details of the calculations

$$\frac{\mathrm{d}\sigma_{\gamma A\to J/\psi A}(t=0)}{\mathrm{d}t} = \frac{\alpha_{em}\sigma^2_{tot,J/\psi A}}{4f^2_{J/\psi}} \; . \tag{7}$$

Constants for the $\gamma p \to J/\psi p$ reaction are obtained from a fit to HERA data: $B_{J/\psi} = 4$ GeV^{-2}, $X_{J/\psi} = 0.0015$ μb, $\epsilon_{J/\psi} = 0.8$ and vector-meson coupling square is $f^2_{J/\psi} = 4\pi \cdot 10.4$.

$$\sigma^{CM}_{tot,J/\psi A} = \int \mathrm{d}^2\mathbf{r}\left(1-\exp\left(-\sigma_{tot,J/\psi p}T_A(\mathbf{r})\right)\right) \; , \tag{8}$$

$$\sigma^{QM}_{tot,J/\psi A} = 2\int \mathrm{d}^2\mathbf{r}\left(1-\exp\left(-\frac{1}{2}\sigma_{tot,J/\psi p}T_A(\mathbf{r})\right)\right) \; , \tag{9}$$

Some details of the calculations

respectively, where r is the distance in the impact parameter space of the photon (or $c\bar{c}$ fluctuation) from the middle of the nucleus-medium and nuclear thickness function is defined as

$$T_A(\mathbf{r}) = \int \rho\left(\sqrt{r^2 + z^2}\right) \mathrm{d}z \; . \tag{10}$$

Formulae (8)-(9) are used to calculate the $\gamma A \to J/\psi A$ cross section.

Some details of the calculations

In our calculation of UPCs we use the following generic formula for the photon flux for any nuclear form factor F

$$N(\omega,b)=\frac{Z^2\alpha_{em}}{\pi^2}\left|\int u^2 J_1(u)\,\frac{F\left(\frac{\left(\frac{\omega b}{\gamma}\right)^2+u^2}{b^2}\right)}{\left(\frac{\omega b}{\gamma}\right)^2+u^2}\right|^2 . \tag{11}$$

Realistic form factor (Fourier transform of the charge density) is used

Centrality classes

In general, centrality of collisions depends on the impact parameter b and a total inelastic nucleus-nucleus cross section

$$c \simeq \frac{\pi b^2}{\sigma_{inel}} \,. \tag{12}$$

In a purely geometrical picture ($\sigma_{inel} = \pi \left(2R_A\right)^2$) we get:

$$c = \frac{b^2}{4R_A^2} \,. \tag{13}$$

We have used the simple formula to describe relation between centrality and impact parameter because, this simpler formula gives almost the same results as that obtained in the Glauber model.

Impact parameter picture

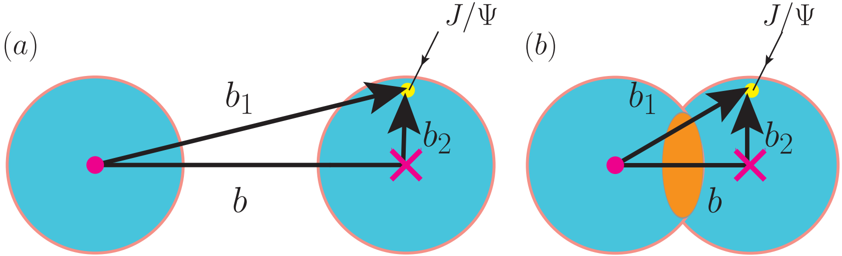

Figure: Impact parameter picture of the collision and the production of the J/ψ meson for ultraperipheral (left panel) and for semi-central (right panel) collisions. It is assumed here that the first nucleus is the emitter of the photon which rescatters then in the second nucleus being a rescattering medium.

Coherent production of J/ψ in b-space

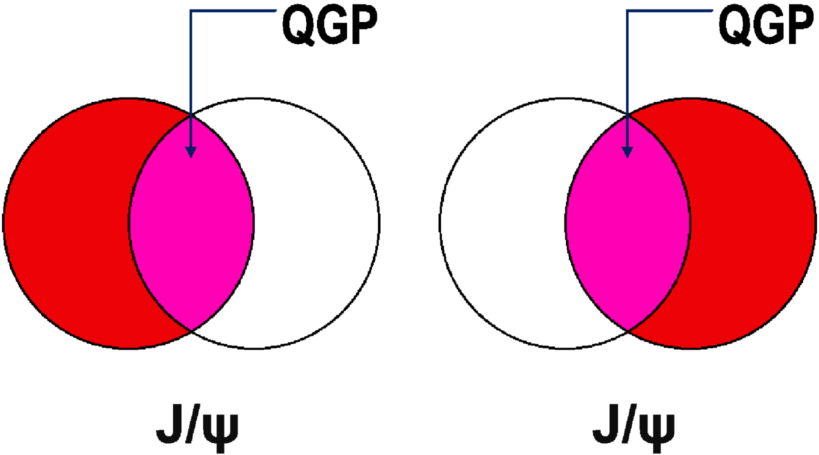

Figure: Picture in the plane x, y perpendicular to the collision axis (z).

Is J/ψ created before nuclear collision ?
Easy to melt J/ψ in the quark-gluon plasma.

Effective fluxes for semicentral collisions

Now we wish to proceed to semi-central collisions i.e. to the case of $b < R_A + R_B$. Then the $S(b)$ factor has to be omitted as we are interested also in situations when colliding nuclei break apart.
The effective photon flux which includes the geometrical aspects can be formally expressed through the real photon flux of one of the nuclei and effective strength for the interaction of the photon with the second nucleus

$$N^{(1)}(\omega_1, b) = \int N(\omega_1, b_1) \frac{\theta(R_A - (|\vec{b_1} - \vec{b}|))}{\pi R_A^2} \mathrm{d}^2 b_1 \,, \qquad (14)$$

where $\vec{b_1} = \vec{b} + \vec{b_2}$. The extra $\theta(R_A - (|\vec{b_1} - \vec{b}|))$ factor ensures collision when the photon hits the nucleus-medium. For the photon flux in the second nucleus one needs to replace 1$\to$2 (and 2$\to$1).
For large $b \gg R_A + R_B$: $N^{(1)}(\omega_1, b) \approx N(\omega_1, b)$. For small impact parameters this approximation is, however, not sufficient.

Effective fluxes for semicentral collsions

Since it is not completely clear what happens in the region of overlapping nuclear densities we suggest another approximation which may be considered rather as lower limit. In this approximation we integrate the photon flux of the first (emitter) nucleus only over this part of the second (medium) nucleus which does not collide with the nucleus-emitter (some extra absorption may be expected in the tube of overlapping nuclei). This may decrease the cross section for more central collisions. In particular, for the impact parameter $b = 0$ the resulting vector meson production cross section will fully disappear by the construction. Then:

$$N^{(2)}\left(\omega_1, b\right) = \int N\left(\omega_1, b_1\right) \frac{\theta(R_A - (|\overrightarrow{b_1} - \overrightarrow{b}|)) \times \theta(b_1 - R_A)}{\pi R_A^2} \mathrm{d}^2 b_1 \,. \tag{15}$$

Some details of the calculations

In our calculations we use also a form factor which is Fourier transform of the charge distribution in nucleus. Two-parameter Fermi distribution of the charge density

$$\rho_{em}(r) = \frac{\rho_{em,0}}{1 + \exp\left(\frac{r-R}{a}\right)} \ , \tag{16}$$

where the density is normalized as

$$\int \rho_{em}(r) \mathrm{d}^3 r = Z \ . \tag{17}$$

Then the normalization constant $\rho_{em,0}$ for the lead nuclei equals to $\frac{Z}{A}0.1604\ \mathrm{fm}^{-3}$ and $R = 6.62$ fm, $a = 0.546$ fm is used in the calculation for charge distribution of the lead nucleus and for the gold nucleus we use: $\rho_{em,0} = \frac{Z}{A}0.1694\ \mathrm{fm}^{-3}$, $R = 6.38$ fm and $a = 0.535$ fm. The form factor (called here realistic form factor) is calculated then as

$$F_{real}(q^2) = \frac{1}{Z}\frac{4\pi}{q} \int \rho_{em}(r) \sin(qr) r \,\mathrm{d}r \ . \tag{18}$$

Impact parameter picture

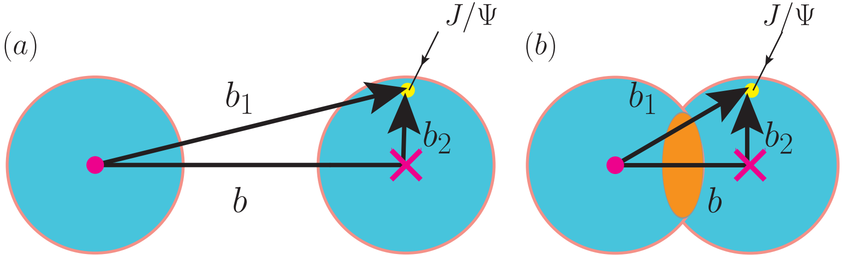

Figure: Impact parameter picture of the collision and the production of the J/ψ meson for ultraperipheral (left panel) and for semi-central (right panel) collisions. It is assumed here that the first nucleus is the emitter of the photon which rescatters then in the second nucleus being a rescattering medium.

Effective fluxes

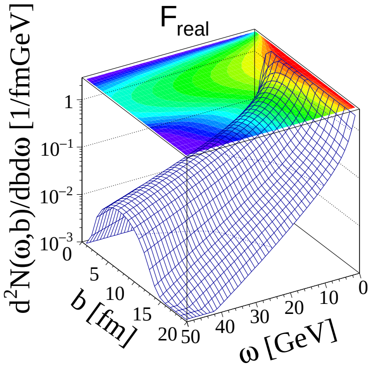

Figure: Standard photon fluxes $N(\omega, b)$ (see Eq. (11)) calculated for realistic (left panel) monopole (right panel) form factors.

Effective fluxes

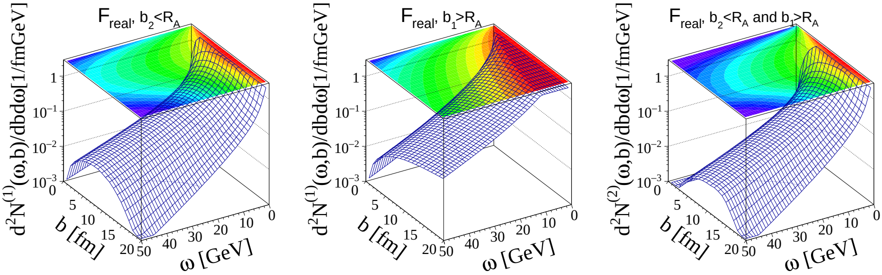

Figure: Two-dimensional distributions of the photon fluxes $N^{(1)}(\omega, b)$ (see Eq. (14)) and $N^{(2)}(\omega, b)$ (see Eq. (15)) in the impact parameter b and in the energy of photon ω for three different conditions (more in the text).

Ratio of fluxes

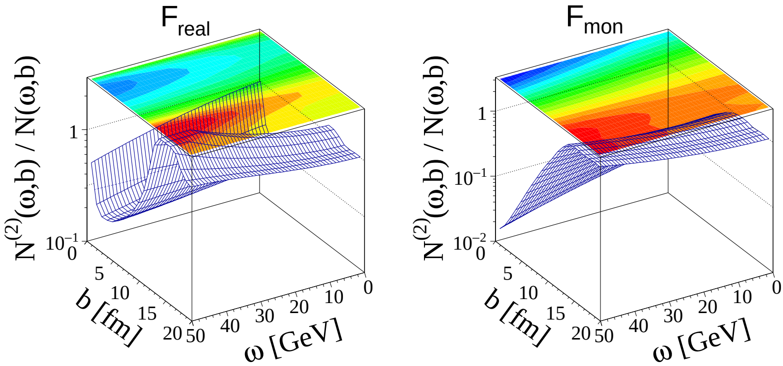

Figure: The ratio of the differential photon fluxes in the impact parameter b and energy of the photon ω. The left panel shows the case with the realistic form factor and the right panel the form factor for monopole form factor.

Centrality of the collisions

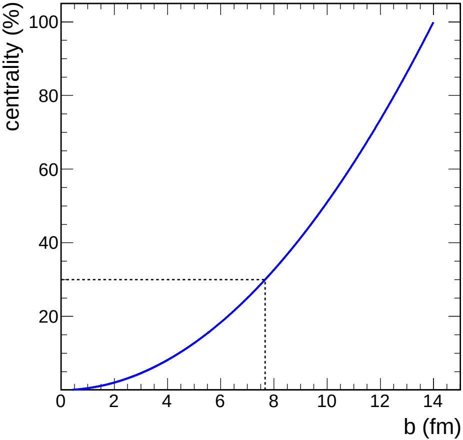

Figure: Centrality of nuclear collisions as a function of the impact parameter as obtained from Eq. (13). For reference we marked $c = 30\%$ and corresponding impact parameter.

Rapidity distribution for UPC

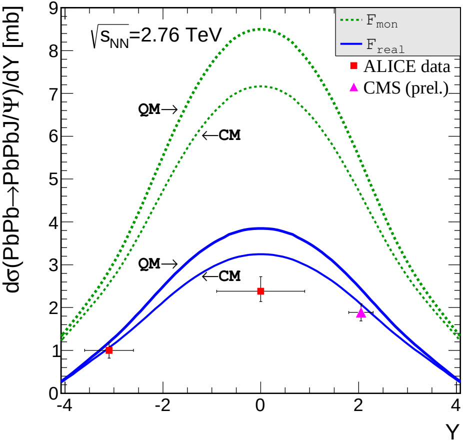

Figure: Differential cross section for coherent production of J/ψ meson in UPC as a function of rapidity of the J/ψ meson compared with the ALICE and CMS data points. We show results for both realistic and monopole form factor, each of them used consistently in Eq. (11) and (3).

Impact parameter dependence

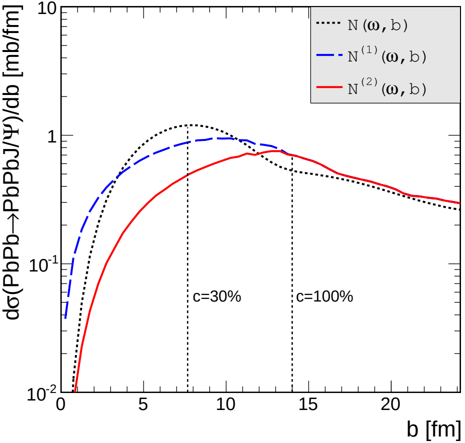

Figure: Differential cross section for photoproduction of J/ψ meson as a function of impact parameter for $\sqrt{s_{NN}} = 2.76$ TeV. Different lines correspond to different approximations: dotted - standard UPC approach (Eq. (11)), dashed - first approximation/correction (Eq. (14)) (upper limit), solid - second approximation/correction (Eq. (15)) (lower limit). Here

Integrated cross section

Flux		Centrality range [%] 30-50	50-70	70-90
$N^{(1)}(\omega,b)$	σ_{tot}^{real} [mb]	2.08	1.60	1.24
$N^{(2)}(\omega,b)$	σ_{tot}^{real} [mb]	1.29	1.21	1.11
	$\mathrm{d}\sigma/\mathrm{d}y$ [μb] ALICE data	73 $\pm 44^{+26}_{-27}$	58 $\pm 16^{+8}_{-10}$	59 $\pm 11^{+7}_{-10}$
$N^{(1)}(\omega,b)$	$\mathrm{d}\sigma^{real}/\mathrm{d}y$ [μb]	160	116	84
$N^{(2)}(\omega,b)$	$\mathrm{d}\sigma^{real}/\mathrm{d}y$ [μb]	91	82	72

Table: Total cross section and the cross section in ALICE rapidity acceptance, $2.5 < y < 4$, for the production of J/ψ in $Pb + Pb$ collisions for $\sqrt{s_{NN}} = 2.76$ TeV calculated with the help of the first $N^{(1)}(\omega,b)$ (Eq. (14)) and second approximation of the photon flux $N^{(2)}(\omega,b)$ (Eq. (15)) for the realistic form factor. The $\frac{\mathrm{d}\sigma}{\mathrm{d}y}$ cross section is compared with the ALICE experimental data.

Comparison to the ALICE data

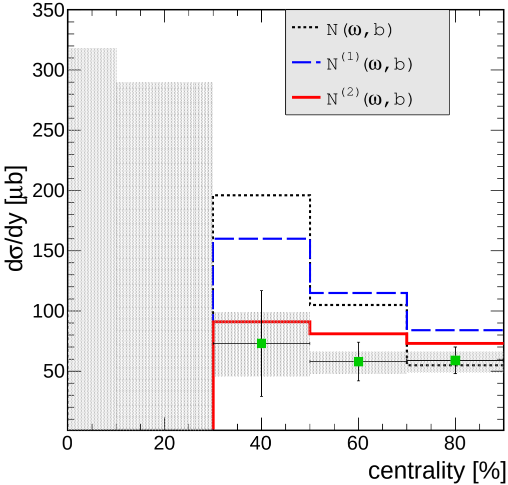

Figure: $\mathrm{d}\sigma/\mathrm{d}y$ cross sections for different centrality bins. Theoretical results for different models of the photon flux are compared with the ALICE data. The shaded area represents the experimental uncertainties.

Photon-Photon Fusion Mechanism

With the nuclear charge form factor F_{em} as an input the flux can be calculated as:

$$N(\omega, b) = \frac{Z^2\alpha_{\mathrm{EM}}}{\pi^2}\left|\int_0^\infty dq_T \frac{q_T^2 F_{\mathrm{em}}(q_T^2 + \frac{\omega^2}{\gamma^2})}{q_T^2 + \frac{\omega^2}{\gamma^2}} J_1(bq_T)\right|^2, \quad (19)$$

where J_1 is a Bessel function. We calculate the form factor from the Fourier transform of the nuclear charge density, for which parameterizations are available.

The differential cross section for dilepton (l^+l^-) production via $\gamma\gamma$ fusion at fixed impact parameter $\boldsymbol{b}$ of a nucleus nucleus collision can then be written as

$$\frac{d\sigma_{ll}}{d\xi d^2\boldsymbol{b}} = \int d^2\boldsymbol{b}_1 d^2\boldsymbol{b}_2\, \delta^{(2)}(\boldsymbol{b} - \boldsymbol{b}_1 - \boldsymbol{b}_2) N(\omega_1, b_1) N(\omega_2, b_2) \frac{d\sigma(\gamma\gamma \to l^+l^-; \hat{s})}{d(-\hat{t})},$$

where the phase space element is $d\xi = dy_+ dy_- dp_{T,l}^2$ with $y_\pm$, $p_{T,l}$ and m_l the single-lepton rapidities, transverse momentum and mass, respectively.

Some details of the calculation

photon energies:

$$\omega_1 = \frac{\sqrt{p_{T,l}^2 + m_l^2}}{2} \left(e^{y_+} + e^{y_-}\right) , \; \omega_2 = \frac{\sqrt{p_{T,l}^2 + m_l^2}}{2} \left(e^{-y_+} + e^{-y_-}\right) , \; \hat{s} = 4\omega_1\omega_2 \, .$$

As can be seen from Eq.(19), the transverse momenta, q_T, of the photons have been integrated out, and dileptons are produced back-to-back in the transverse plane, *i.e.* , the transverse momentum P_T of the pair is neglected.

In UPCs the incoming nuclei do not touch, *i.e.* , no strong interactions occur between them. In this case one usually imposes the constraint $b > 2R_A$ when integrating over impact parameter $b = |\boldsymbol{b}|$.

Coherent production of l^+l^- in b-space

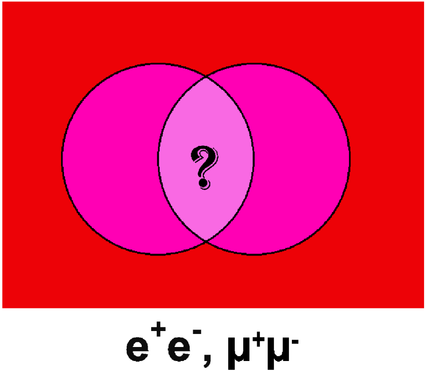

Figure: Picture in the plane x, y perpendicular to the collision axis (z).

Is e^+e^- created before nuclear collision ?
Can plasma/spectators distort distributions of leptons ?
Here not big difference between UPC and non-UPC.

Some details of the calculation

Here we lift this restriction allowing the nuclei to collide. Then the dileptons will be produced on top of the hadronic nuclear event characterized by an impact parameter $\boldsymbol{b}$. Note that even for overlapping nuclei, $b < 2R_A$, leptons are predominantly produced outside the overlap region, for $b_{1,2} > R_A$. This situation is very different from the photoproduction heavy vector mesons which tend to be produced inside of one of the nuclei.

The mass-differential dilepton yield from coherent photons in a centrality class $\mathcal{C}$ corresponding to an impact parameter range of $[b_{\rm min}, b_{\rm max}]$ can be calculated as:

$$\frac{dN_{ll}[\mathcal{C}]}{dM} = \frac{1}{f_{\mathcal{C}} \cdot \sigma_{\rm AA}^{\rm in}} \int_{b_{\rm min}}^{b_{\rm max}} db \int d\xi\, \delta(M - 2\sqrt{\omega_1 \omega_2})\, \frac{d\sigma_{ll}}{d\xi db}\Big|_{\rm cuts}\,, \qquad (22)$$

where we have indicated kinematic cuts on single-lepton variables as applied in experiment, and $f_{\mathcal{C}}$ is the fraction of inelastic hadronic events contained in the centrality class $\mathcal{C}$.

Some details of the calculation

$$f_{\mathcal{C}} = \frac{1}{\sigma_{\rm AA}^{\rm in}} \int_{b_{\rm min}}^{b_{\rm max}} db \frac{d\sigma_{\rm AA}^{\rm in}}{db} \,. \tag{23}$$

We determine $[b_{\rm min}, b_{\rm max}]$ and $\sigma_{\rm AA}^{\rm in}$ by using the optical Glauber model as

$$\frac{d\sigma_{\rm AA}^{\rm in}}{db} = 2\pi b(1 - e^{-\sigma_{\rm NN}^{\rm in} T_{\rm AA}(b)}) \,. \tag{24}$$

The nuclear thickness function, $T_{\rm AA}(b)$, is obtained from the convolution of nuclear density distributions for which we use standard Woods-Saxon profiles, $n_{\rm A}(r)$,

$$T_{\rm AA}(b) = \int d^3\vec{r}_1 d^3\vec{r}_2 \, \delta^{(2)}(\boldsymbol{b} - \boldsymbol{r}_{1\perp} - \boldsymbol{r}_{2\perp})\, n_{\rm A}(r_1) n_{\rm A}(r_2) \,. \tag{25}$$

Some details of the calculation

An exact calculation of the pair-P_T dependence is, in general, rather involved especially for finite impact parameter(s), (see, *e.g.* , Vidovic et al.,Hencken et al.). Here we perform a simplified calculation using b-integrated momentum dependent photon fluxes,

$$\frac{dN(\omega, q_T^2)}{d^2\vec{q}_T} = \frac{Z^2\alpha_{EM}}{\pi^2}\frac{q_T^2}{[q_T^2 + \frac{\omega^2}{\gamma^2}]^2}F^2_{\mathrm{em}}(q_T^2 + \frac{\omega^2}{\gamma^2}). \tag{26}$$

The P_T distribution is then obtained as the convolution of two transverse momentum dependent photon fluxes with the elementary $\gamma\gamma \to e^+e^-$ cross section,

$$\frac{d\sigma_{ll}}{d^2\vec{P}_T} = \int \frac{d\omega_1}{\omega_1}\frac{d\omega_2}{\omega_2}d^2\vec{q}_{1T}d^2\vec{q}_{2T}\frac{dN(\omega_1, q_{1T}^2)}{d^2\vec{q}_{1T}}\frac{dN(\omega_2, q_{2T}^2)}{d^2\vec{q}_{2T}}\delta^{(2)}(\vec{q}_{1T}+\vec{q}_{2T}-\vec{P}_T)\hat{\sigma}(\tag{27}$$

The resulting shape of integrated cross section is then re-normalized to the previously obtained cross section for a given centrality class.

Other sources of dileptons

- Thermal emission in QGP
  $q\bar{q} \to l^+l^-$, $T = T(\tau)$
- $\rho^0 \to l^+l^-$, modified in the medium
- so called coctail
  - Dalitz decays
    $\pi^0, \eta, \eta' \to e^+e^-\gamma$, $\Delta^+ \to pe^+e^-$
  - $V \to l^+l^-$
  - Drell-Yan NN colissions
  - double (simultaneous) semi-leptonic decays of D and $\bar{D}$ mesons

  (Data driven calculation (STAR))
- Coherent $V \to l^+l^-$
  (not included here)

Thermal Dileptons and modified ρ^0, a sketch

Thermal dilepton radiation in URHICs is based on the idea that the abundant production of hadrons, together with strong re-interactions, leads to the formation of locally near-equilibrated medium whose expansion can be described by relativistic viscous hydrodynamics. This idea is by now well established, on the one hand by the success of hydrodynamic modelling in reproducing the transverse-momentum spectra of the produced hadrons and by the observation and theoretical description of dilepton radiation that goes well beyond the final-state decays of the produced hadrons (Rapp et al.).

To compute dilepton invariant-mass spectra an integration of the thermal emission rate over the space-time evolution of the expanding fireball is performed,

$$\frac{dN_{ll}}{dM} = \int d^4x \; \frac{M d^3P}{P_0} \; \frac{dN_{ll}}{d^4x d^4P} \,, \tag{28}$$

where $(P_0, \vec{P})$ and $M = \sqrt{P_0^2 - P^2}$ are the 4-vector ($P = |\vec{P}|$) and invariant mass of the lepton pair, respectively.

Thermal Dileptons and modified ρ^0, a sketch

The thermal emission rate,

$$\frac{dN_{ll}}{d^4x d^4P} = -\frac{\alpha_{\rm EM}^2 L(M)}{\pi^3 M^2}\, f^B(P_0;T)\ {\rm Im}\Pi_{\rm EM}(M,P;\mu_B,T)\ , \qquad (29)$$

is expressed in terms of the Bose distribution function, f^B, and the EM spectral function, Im $\Pi_{\rm EM}$, depending on the local temperature, T, and baryon chemical potential, μ_B, of the medium (the lepton phase-space factor, $L(M)$, approaches one for $M \gg m_l$). The fireball medium generally evolves through both QGP and hadronic phases (pre-equilibrium phases contribute negligibly to soft radiation). For the respective spectral functions we employ in-medium quark-antiquark annihilation constrained by lattice-QCD (Rapp et al.) and in-medium vector spectral functions in the hadronic sector.

Dileptons from fireball

- The vector meson resonances strongly broaden in the medium and essentially melt at temperatures close to the pseudocritical one, providing a nearly smooth transition to the QGP rates.
- Different centrality classes for different colliding systems are characterized by the measured hadron multiplicities and appropriate initial conditions for the fireball.
- For the purpose of computing EM radiation in URHICs, simple fireball models have been employed (Rapp et al.) utilizing a relativistic volume expansion with acceleration parameters inferred from hydrodynamic models as well as dilepton P_T spectra.
- Here we employ the model of van Hees et al.(2007). with an updated equation of state (EoS) (Rapp et al.) consistent with lattice-QCD results for the QGP, smoothly matched to a hadron resonance gas (the dilepton mass spectra a rather insensitive to the EoS update).
- This approach is consistent with available dilepton data from SIS, SPS and RHIC energies

Au-Au Collisions at RHIC

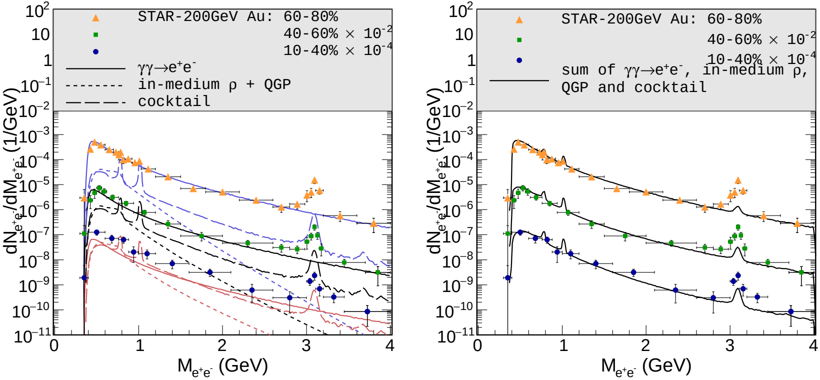

Figure: Left: Dielectron invariant-mass spectra for pair-$P_T < 0.15$ GeV in Au+Au($\sqrt{s_{NN}}$=200 GeV) collisions for 3 centrality classes including experimental acceptance cuts ($p_{T,e} > 0.2$ GeV, $|\eta_e| < 1$ and $|y_{e^+e^-}| < 1$) for $\gamma\gamma$ fusion (solid lines), thermal radiation (dotted lines) and the hadronic cocktail (dashed lines); right panel: comparison of the total sum (solid lines) to STAR data.

Au-Au Collisions at RHIC

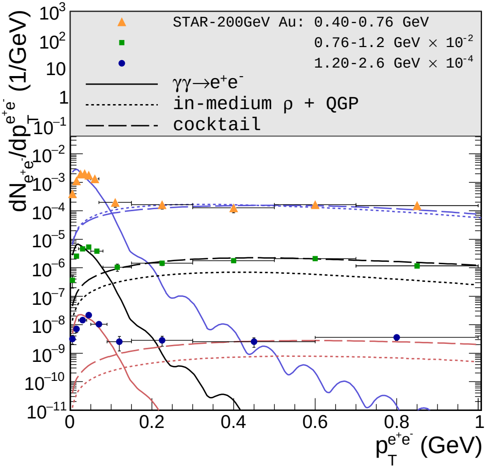

Figure: P_T spectra of the individual contributions (line styles as in the previous figure) in 3 different mass bins for 60-80% Au+Au($\sqrt{s_{NN}}$=200 GeV), compared to STAR data.

In+In Collisions at the SPS

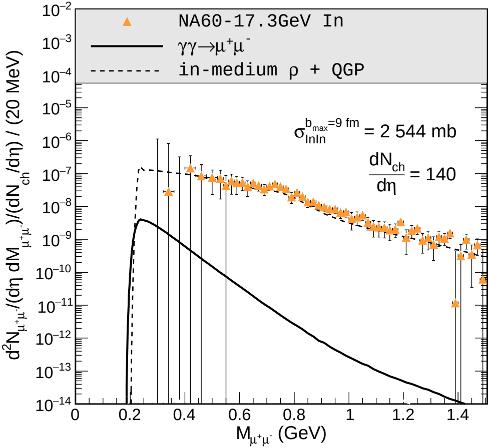

Figure: Low-P_T (<0.2 GeV) acceptance-corrected dimuon invariant mass excess spectra in the rapidity range 3.3<$Y_{\mu^+\mu^-,LAB}$<4.2 for MB In+In ($\sqrt{s_{NN}}$=17.3 GeV) collisions at the SPS. Calculations for coherent $\gamma\gamma$ fusion (solid line) and thermal radiation (dashed line) are compared to NA60 data.

Pb+Pb Collisions at the LHC

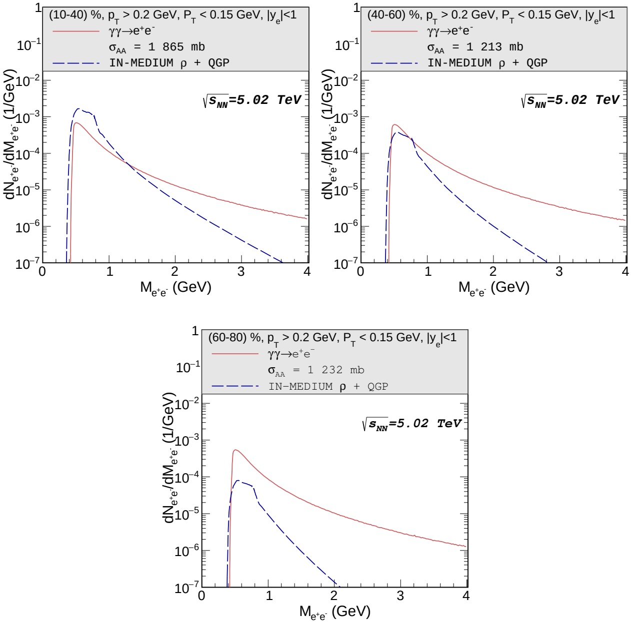

Excitation Function

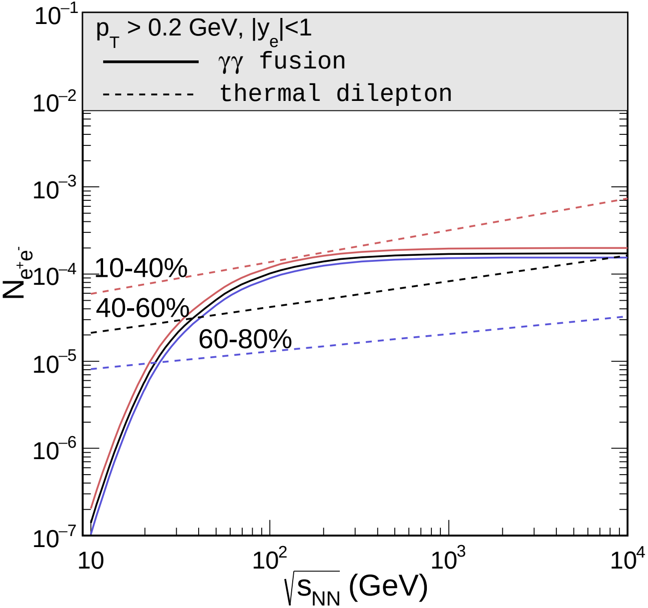

Conclusions

- We have shown that photoproduction of J/ψ meson survives also for peripheral and semicentral collisions and gives contribution at small J/ψ transverse momenta.
- We have shown how to change fluxes (in the impact parameter space) to describe ALICE data for different ranges of centrality.
- We have shown that dielectron invariant mass distributions with the restriction on low dielectron transverse momenta can be described (with correct normalization) using the $\gamma\gamma \to e^+e^-$ mechanism for broad range of centralities.
- We have described also the shape of transverse momentum enhancement in $p_{t,sum}$ for different centralities.
- We have compared energy dependence of the $\gamma\gamma \to e^+e^-$ and thermal mechanisms as a function of collision energy and found that RHIC energies are optimal for $\gamma\gamma \to e^+e^-$.
- More precise analysis of the low-$p_{t,sum}$ enhancement could test EM effects of spectators and participant zone so could provide some information on space-time picture of the reaction.

Outlook

- Calculate b-dependent and transverse momentum dependent photon fluxes.
- Study also $d\sigma/d\phi_{\mu\mu}$ (new ATLAS data)).
- Include simultaneously continuum and vector mesons.

Outlook

- Calculate *b*-dependent and transverse momentum dependent photon fluxes.
- Study also $d\sigma/d\phi_{\mu\mu}$ (new ATLAS data)).
- Include simultaneously continuum and vector mesons.

Thank You